ELSEVIER

European Journal of Pharmaceutical Sciences 14 (2001) 281–291

EUROPEAN JOURNAL OF PHARMACEUTICAL SCIENCES

www.elsevier.nl/locate/ejps

pH-metric solubility. 3. Dissolution titration template method for solubility determination☆

Alex Avdeef*, Cynthia M. Berger

pION Inc., 5 Constitution Way, Woburn, MA 01801, USA

Received 2 February 2001; received in revised form 28 June 2001; accepted 12 July 2001

Abstract

The main objective of this study was to develop an effective potentiometric saturation titration protocol for determining the aqueous intrinsic solubility and the solubility–pH profile of ionizable molecules, with the specific aim of overcoming incomplete dissolution conditions, while attempting to shorten the data collection time. A modern theory of dissolution kinetics (an extension of the Noyes–Whitney approach) was applied to acid–base titration experiments. A thermodynamic method was developed, based on a three-component model, to calculate interfacial, diffusion-layer, and bulk-water reactant concentrations in saturated solutions of ionizable compounds perturbed by additions of acid/base titrant, leading to partial dissolution of the solid material. Ten commercial drugs (cimetidine, diltiazem hydrochloride, enalapril maleate, metoprolol tartrate, nadolol, propoxyphene hydrochloride, quinine hydrochloride, terfenadine, trovafloxacin mesylate, and benzoic acid) were chosen to illustrate the new titration methodology. It was shown that the new method is about 10 times faster in determining equilibrium solubility constants, compared to the traditional saturation shake-flask methods. © 2001 Elsevier Science B.V. All rights reserved.

Keywords: Solubility; Dissolution; Solubility-ph profile; Potentiometric; Titration; Oral absorption

1. Introduction

In the measurement of aqueous solubility of ionizable substances, complications of solution chemistry, such as incomplete dissolution (Higuchi et al., 1979; Venkatesh et al., 1996), supersaturation (Ledwidge and Corrigan, 1998), complexation reactions (Ritschel et al., 1983), aggregation reactions (Bogardus and Blackwood, 1979; Streng et al., 1996), micelle formations (Roseman and Yalkowsky, 1973; Attwood and Gibson, 1978), the effects of common ions (Miyazaki et al., 1981), buffers (Mooney, 1980; Mooney et al., 1981a,b), and microclimates (Serajuddin and Jarowski, 1985a,b), can make solubility assessment problematic and incomplete. In recent literature, differences of an order of magnitude in reported solubilities are not rare. New methods of solubility determination, based on improved understanding of solution chemistry and employing more general and rigorous mathematical treatments of data, may help to improve the quality of 'difficult' measurements, and if so, may be welcome.

We have been developing a new solubility technique, as an alternative to the traditional shake-flask method, based on potentiometric dissolution titrations (Avdeef, 1998; Avdeef et al., 2000). Although determination of solubility by potentiometry is quite uncommon, interest in it has been growing (Levy and Rowland, 1971; Roseman and Yalkowsky, 1973; Charykov and Tal'nikova, 1974; Kaufman et al., 1975; Streng and Zoglio, 1984; Todd and Winnike, 1994; Strafford et al., 2000; Faller and Wohnsland, 2001). In our approach, the theoretical framework for the equilibrium data processing is based on the use of complete mass-balance equations, coupled with a unique use of Bjerrum plots (Avdeef, 1998) to approximate intrinsic solubility constants, and followed by rigorous nonlinear least-squares analysis to refine them (Avdeef, 1985, 1998; Avdeef et al., 2000). The generality of the method makes it suitable to tackle many complexities of solution chemistry. The initial results of the new solubility–pH method have been successfully compared to those obtained by traditional methods (Avdeef et al., 2000; Strafford et al., 2000), and an optimistic assessment has been presented (Faller and Wohnsland, 2001). In the draft

☆Avdeef et al. (2000) is Part 2 of the series.

*Corresponding author. Tel.: +1-781-935-8939; fax: +1-781-935-8938.

E-mail address: aavdeef@pion-inc.com (A. Avdeef).

0928-0987/01/$ – see front matter © 2001 Elsevier Science B.V. All rights reserved.
PII: S0928-0987(01)00190-7

document describing FDA's Biopharmaceutics Classification System, the new acid–base titration method is deemed suitable for the determination of solubility (FDA, 1999).

In the present study, we use the theory of kinetics of dissolution of ionizable compounds (an expansion of the Noyes–Whitney approach) applied to titrated solutions to demonstrate that the new pH-metric method, in the way it has been optimized, is at least an order of magnitude faster than the traditional shake-flask solubility methods. In the new method the pH is adjusted with acid or base titrants; auxiliary buffers are *not* used. We illustrate this with 10 commercial drugs.

2. Theoretical section

2.1. Dissolution kinetics applied to titrations

In acid–base dissolution titrations of ionizable compounds, the titrant perturbs the saturated system at equilibrium and causes a portion of the suspended solid to dissolve (taking the system out of equilibrium), a process which can be very slow, depending on a number of factors. In order to collect pH data suitable for the reliable determination of solubility constants, it is necessary to allow the titrated system to return to an equilibrium state following each titrant addition.

The relationship between the rate of dissolution, dm/dt, and the solubility, C_S, is described by the Noyes–Whitney equation (Noyes and Whitney, 1897)

$$dm/dt = A(D/h)(C_S - C) \quad (1)$$

where m is mass (mol), t is time (s), C is concentration of solute dissolved at a particular time (mol/cm^3), C_S is equilibrium solubility (mol/cm^3), D is diffusivity (cm^2/s), h is apparent thickness (cm) of the diffusion layer (depends on rate of stirring and the temperature), and A is surface area available for dissolution (cm^2). The less soluble the titrated substance, the longer it takes the system to re-establish equilibrium following titrant perturbations; the closer the system is to complete dissolution ($C \approx C_S$), the slower is the dissolution process.

According to the Nernst–Brünner diffusion layer model (Nernst, 1904; Brünner, 1904), the outermost layer of the solid compound dissolves very quickly into a thin layer of solvent to form a saturated solution adjacent to the surface, and a steady state of material flows into the bulk solution. For diffusion layer thicknesses of 10–100 μm and drug diffusivities about 5×10^{-6} cm^2/s, the time to reach steady state is approximately 0.02–2 s (Weiss, 1996). By steady state, it is meant that the total concentration (at a particular time) changes linearly with position across the diffusion layer.

When dissolving ionizable compounds undergo simultaneous chemical reactions, such as ionization (Mooney, 1980; Mooney et al., 1981a,b), Eq. (1) needs to be qualified. The rate can depend dramatically on the pH of the titrated solution and the presence of buffers. To develop an optimized data collection algorithm (i.e., one that is as fast as the rate of dissolution permits), it was necessary to consider the relationship between intrinsic solubility, pH, and the rate of dissolution.

In their comprehensive work with the dissolution kinetics of ionizable weak acids, Mooney (1980) and Mooney et al. (1981a,b) have developed critical extensions of Noyes–Whitney equation. Later, Serajuddin and Jarowski (1985a,b) considered weak bases and hydrochloride salts and proposed that the Noyes–Whitney equation in its simplest form (Eq. (1)) did not correctly predict the observed fluxes of ionizable substances under certain circumstances. It was necessary to consider the concentrations of species in the diffusion layer, at the solid–liquid interface, rather than solely in the bulk solution in order to rationalize the observed dissolution rates (Mooney et al., 1981a,b; Serajuddin and Jarowski, 1985a,b). To explore the dynamics of dissolution titrations, we adapted the steady-state kinetics model of Mooney (1980) and Mooney et al. (1981a,b), but with the following modification. Since it makes no sense to assume a sink condition in a dissolution titration, the boundary conditions had to be changed, which led to slightly different equations. Consider the following system of reactions of a weak base, titrated with HCl from high pH to low pH.

$$B + H^+ \rightleftarrows BH^+ \quad (2)$$

$$B + H_2O \rightleftarrows BH^+ + OH^- \quad (3)$$

$$B \rightleftarrows B(s) \quad (4)$$

The corresponding mass balance equations in the aqueous phase are

$$T_B(x,t) = [B] + [BH^+] \quad (5)$$

$$T_H(x,t) = [H^+] - [OH^-] + [BH^+] \quad (6)$$

where the brackets denote concentrations of reactants. T_B and T_H are the total concentrations of the weak base and the hydrogen excess, respectively, as functions of position x and time t. In our presentation, the *initial* steady-state rate of dissolution, shortly following titrant addition, will be evaluated. (Mooney used a pH-stat to maintain a constant rate of dissolution at a fixed pH, hence a constant steady state; also his equations were derived with an assumed sink condition.) In a titration experiment, the pseudo-steady-state rate decreases with time, as bulk-solution pH changes and a new equilibrium state forms.

From Fick's first law of diffusion, the steady-state flux (mol/cm^2 s) is

$$J = -D(dC/dx) = (dm/dt)/A = V/A(dC/dt) \quad (7)$$

Differentiation of Eqs. (5) and (6) with respect to time and applying Fick's law, Eq. (7), produces the initial (maximum) steady-state rate of dissolution. Following the steps leading to Mooney's Eqs. (23) and (24) (1980), the solutions to the differential expressions can be stated as

$$D_B [B] + D_{BH}[BH^+] = c_1 x + c_3 \quad (8)$$

$$D_H[H^+] - D_{OH}[OH^-] + D_{BH}[BH^+] = c_2 x + c_4 \quad (9)$$

with integration constants c_1–c_4. The D-terms refer to diffusivities of the various reactants. Two sets of boundary concentrations may be considered to solve the above equations. One set consists of all of the equilibrium reactant concentrations at $x=0$, in the diffusion layer adjacent to the surface of the solid, and another set consists of reactant concentrations at $x \geq h$, at $t=0$ (after titrant added but before dissolution started). The former set is labeled $[B]_0$, $[BH^+]_0$, $[H^+]_0$, and $[OH^-]_0$, while the latter set is labeled $[B]_h$, $[BH^+]_h$, $[H^+]_h$, and $[OH^-]_h$. Substitutions of the boundary conditions into Eqs. (8) and (9) eliminate some of the integration constants and produce the relationships

$$c_1 = -\{D_B([B]_0 - [B]_h)/h + D_{BH}([BH^+]_0 - [BH^+]_h)/h\} \quad (10)$$

$$c_2 = -\{D_H([H^+]_0 - [H^+]_h)/h - D_{OH}([OH^-]_0 - [OH^-]_h)/h + D_{BH}([BH^+]_0 - [BH^+]_h)/h\} \quad (11)$$

The initial total flux of the dissolving substance is expressed by Eq. (10). We can make the approximation that $D_B \approx D_{BH}$ (as suggested by the Stokes–Einstein equation, Mooney, 1980) and obtain the initial-state dissolution flux expression

$$\begin{aligned} dm/dt &= A(D_B/h)([B]_0 - [B]_h + [BH^+]_0 - [BH^+]_h) \\ &= A(D_B/h)\,(T_B^0 - T_B^h) \end{aligned} \quad (12)$$

We now need to calculate the reactant concentrations at $x=0$ and h, to solve the dissolution rate expression (Eq. 12). The approach we use is completely different from that described by Mooney. We adapted well-tested general equilibrium analysis, as described by Avdeef (1985, 1998), to a 'three-state model,' described below.

2.2. Three-state model: calculation of interfacial and bulk solution reactant concentrations

In this section our specific objective is to come up with a general way to calculate the equilibrium concentrations of all reactants (e.g., $[B]_0$, $[BH^+]_0$, $[H^+]_0$, $[OH^-]_0$, $[B]_h$, $[BH^+]_h$, $[H^+]_h$, and $[OH^-]_h$) for any given system of equations (with any of the complexities mentioned in the introduction) under three types of conditions: (a) at equilibrium before titrant addition, where the concentrations of reactants are the same in the diffusion layer and the bulk solution, (b) in the bulk-water solution immediately after titrant addition and thorough mixing, but before any subsequent solid dissolution ($t=0$), and (c) in the diffusion layer immediately adjacent to the solid surface, the moment steady-state is reached ($t \leq 2$ s), but before any significant amount of dissolution takes place (maximum gradient, dC/dx, in the diffusion layer). These three states are depicted in Fig. 1: cases (a), (b), and (c), along with case (d) representing the consequent equilibrium state ($t=\infty$). In the figure, a very simple model was used, consisting of a weak base in an alkaline solution with pH near the pK_a.

To proceed, two equilibrium states, Σ_i and Σ_0 may be defined in a dissolution titration. The *initial* state Σ_i is transformed into the *final* state Σ_0 by the addition of a specific amount of titrant, τ. Furthermore, the titrant is selected to cause the pH to change in the direction of dissolution (i.e., the state Σ_0 has less solid than the state Σ_i). The concentrations of all species in the two states can be calculated, without invoking any kinetic considerations. The computer program we used, *p*S (see Section 3), is able to calculate concentrations of all species at equilibrium in a saturated solution. It is necessary only to specify all of the pertinent equilibrium constants and the total concentrations of reactants. Fig. 1 shows the two equilibrium states as (a) and (d).

Consider a third state, Σ_h, which is defined by the following 'thought' experiment. The residual solid suspended in solution in state Σ_i is temporarily 'removed' to obtain the supernatant aqueous solution. To this solution, τ amount of titrant is added (the same quantity which takes Σ_i to Σ_0). No precipitate forms, since the titrant takes the system further away from saturation. The perturbed homogeneous system quickly equilibrates, to state Σ_h. This is depicted in block (b) in Fig. 1. All concentrations in this state are calculated by *p*S, as before. Now consider instantaneously re-suspending the solid which had been removed in the thought experiment. The liquid film that quickly surrounds the solid rapidly equilibrates to the conditions of state Σ_0 (block (c) in Fig. 1). A considerably slower process follows: the bulk solution, beyond the thin film at the solid–liquid interface, relaxes from state Σ_h to state Σ_0, as solid dissolves (depicted by the disappearance of the lightly shaded block in frame (d) in Fig. 1) to establish the final equilibrium state.

Since T_B in states Σ_i and Σ_h are the same (since the solid is 'removed' during the calculation step associated with Σ_h), Eq. (12) may be simplified by substituting $T_B^0 - T_B^i$ for $T_B^0 - T_B^h$ and noting $[B]_0 = [B]_i$ (in a saturated solution, [B] is the intrinsic solubility of the uncharged species) to obtain

$$dm/dt = A(D_B/h)\,([BH^+]_0 - [BH^+]_i) \quad (13)$$

A numerical example of the use of Eq. (13) will be given in Section 4.

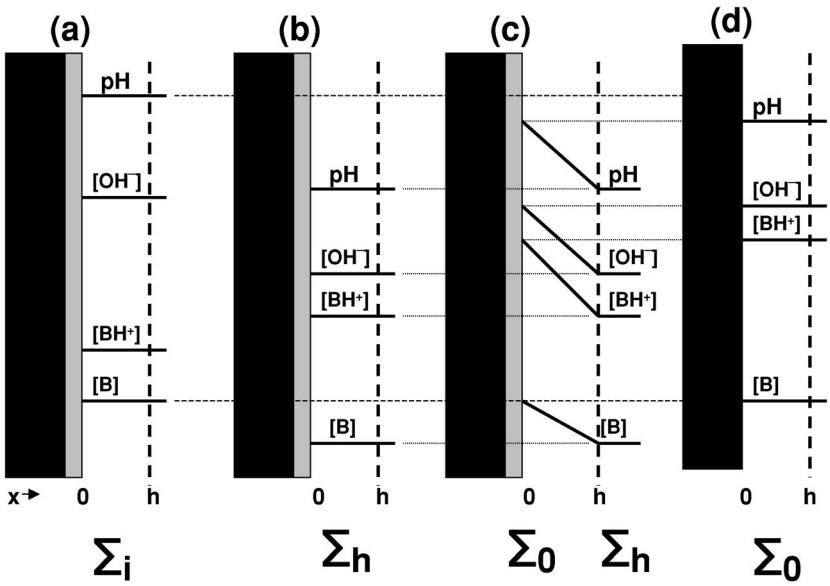

Fig. 1. Schematic representing the three-state model (see text). Depicted is the case of a weak base, B, titrated with HCl in an alkaline solution at a pH near the pK_a. The vertical direction represents concentration of reactants; the horizontal direction represents distance from the surface of the solid. The solid is represented by rectangles. The lighter shaded rectangle represents the amount of solid which dissolves as a result of HCl titrant addition. Block (a) represents the initial state, Σ_i, before titrant addition. Block (b) represents the situation right after titrant addition, where the bulk solution is equilibrated by convective mixing, but none of the solid has dissolved ($t=0$). Block (c) represents the equilibration of the solution adjacent to the surface of the solid and the establishment of the initial steady state ($t \leq 2$ s). Block (d) represents the equilibrium state ($t=\infty$), where a portion of the solid has been dissolved, and a lower-pH solution has been formed. The transition from states (a) to (b) is nearly instantaneous; from (b) to (c) takes less than 2 s; from (c) to (d) takes minutes or hours. The vertical dashed lines represent the boundary between the diffusion layer and bulk solution. The horizontal dashed lines assist in visualizing that pH has decreased in block (d) compared to block (a), but that the concentration of the uncharged (free) base has remained the same in (d) as in (a), as is characteristic of a saturated solution.

3. Materials and methods

3.1. Materials

The preparation and standardization of titrants (0.5 M HCl and 0.5 M KOH) and the special calibration of the pH electrode are described elsewhere (Avdeef, 1998; Avdeef and Bucher, 1978). Cimetidine, diltiazem hydrochloride, enalapril maleate, metoprolol tartrate, nadolol, propoxyphene hydrochloride, quinine hydrochloride, and terfenadine were obtained from Sigma (St. Louis, MO, USA), and used as received. Benzoic acid was obtained from Aldrich (Milwaukee, WI, USA). Trovafloxacin mesylate was obtained from Pfizer Research (Groton, CT). The compounds were confirmed to be of high purity by potentiometric analysis. The distilled water used in the study was purified in a continuously recirculating mixed-bed ion-exchange/organic filter system (Barnstead, Model EASYpure RF).

3.2. Apparatus

The potentiometric solubility data were obtained with the *p*SOL Model 3 instrument (*p*ION Inc., Woburn, MA, USA) and subsequently processed with the accompanying computer program, *p*S. The new solubility instrument is equipped with three precision dispensers (capable of adding a minimum volume of 0.02 μl) and a high-impedance (10^{15} Ω) pH circuit. A semi-micro combination pH electrode (Ag/AgCl, annular ring single junction) was used (*p*ION Inc.). The saturation titrations were performed in a test tube jacketed by a glass vessel with thermostated water circulating through it, keeping the temperature constant at 25°C. A teflon-coated magnetic stir bar was used to agitate the titrated solution. A blanket of argon gas gently flowed over the solution. Titrated solution volumes ranged from 1.7 to 5 ml, but were usually less than 3 ml. The assay can accommodate sample weights as low as 50–100 μg (depending on the solubility of the sample). A background electrolyte, 0.15 M KCl, was used to lessen the effect of small changes in ionic strength due to sample and titrant additions and to improve the electrode performance. Care was taken to ensure that the amount of sample used was less than a thousand times the predicted (Eq. (14)) minimum sample solubility, to avoid chloride or potassium salt precipitation of the drug, due to the background electrolyte.

The ionization constants (pK_a) and the octanol–water partition coefficients ($\log P_{ow}$) of the compounds were measured using the GLpKa instrument (Sirius Analytical Instruments, Forest Row, E. Sussex, UK).

3.3. Dissolution titration template (DTT)

The *p*SOL is principally distinguished from ordinary titrators by a uniquely unusual data collection regime, based on the use of pre-calculated titration curves serving as templates. The instrument takes as input parameters the pK_a and the octanol–water partition coefficient ($\log P_{ow}$) of the sample. Values calculated by any of several commercial software programs suffice. However, measured pK_a and $\log P_{ow}$ values are more likely to enhance the efficiency of the data collection process. (If the constants are not provided, the instrument resorts to collecting data in the manner of an ordinary titrator). The $\log P_{ow}$ parameter is provided for estimating the intrinsic solubility, S_0, according to the simple linear expression

$$\log S_o = 1.17 - 1.38 \log P_{ow} \quad (14)$$

one of several described in Yalkowsky and Banerjee's book (1992). Using the pK_a and the estimated S_0, the instrument calculates (Avdeef, 1985, 1998) the entire titration curve (pH versus volume of titrant, e.g., Fig. 2) *before* starting the assay. The curve serves as a template from which the instrument 'learns' how to collect individual pH measurements in the course of the titration.

Enough sample is weighed (template-based recommendations are made by the instrument) to cause precipitation during some portion of the titration. The pH where precipitation takes place is known from the template simulation (Avdeef, 1998), and data collection strategy is set accordingly, as described below. For compounds with predicted $S_0 < 500$ μg/ml, the solid is first rapidly dissolved in either strong acid or strong base, then quickly re-precipitated and stirred for about 10–60 min, depending on predicted S_0, before the actual titration starts (during which time crystals often form out of the turbid suspension as can be visually evident with the aid of a magnifying glass). It should be noted that polymorph of the compound can change as a result of this step. Titrations of weak acids begin at low pH and those of weak bases begin at high pH. KOH (or HCl) titrant is dispensed accurately and slowly into the slurry, to drive the pH of the solution in the direction of dissolution, eventually well past the point of complete dissolution.

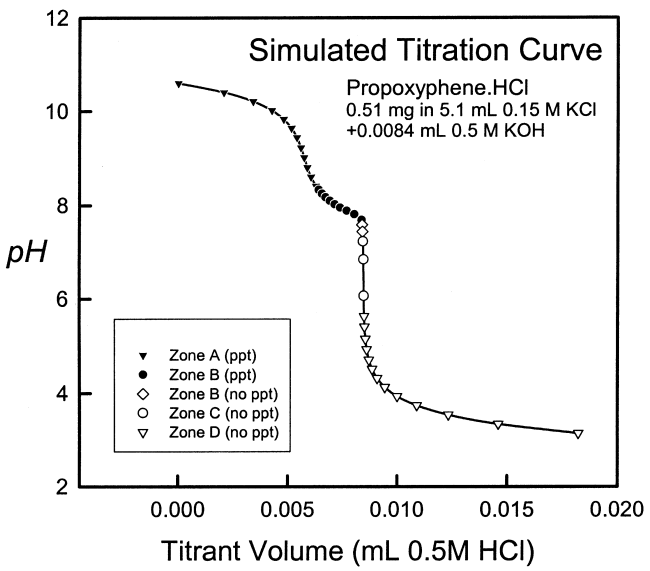

Fig. 2. Template simulation for 0.51 mg propoxyphene hydrochloride in 5.1 ml 0.15 M KCl, using the pK_a 9.06 and $\log P_{ow}$ 4.37.

As titrant is added, careful measurements of pH are made. The instrument dramatically slows down the rate of data taking as the point of complete dissolution approaches in the titration. The *p*SOL uses the dissolution rate expression, Eq. (13), with reactant concentrations calculated on the basis of the template model, to estimate how long to wait for equilibrium to be reached following the addition of titrant. Consequently, some data are collected at moderate speeds and some at very slow speeds. For example, about 20% of the data, nearest the pH region of complete dissolution, are allotted about 80% of the total titration time. In this way, problems of incomplete dissolution are minimized, or at least are easily identified by the shape of the resultant distortion in the actual titration curve (also indicated by the high weighted residuals in that region in the least-squares refinement of constants described below). Only after the precipitate completely dissolves (assessment based on the template prediction), does the instrument collect the remainder of the data rapidly, as would regular titrators. Typically, 4–10 h are required for the entire equilibrium solubility data taking. The more insoluble the compound is anticipated to be (based on the template) the longer the recommended assay time. In an ideally designed assay (i.e., when the template is accurate to ±0.5 log unit in estimated intrinsic solubility), only a single titration is needed to determine the intrinsic solubility constant and the entire solubility–pH profile. We call this novel pH-metric protocol the dissolution titration template (DTT) method.

3.4. Bjerrum difference plots

The Bjerrum difference plots are useful graphical tools in solution equilibrium analysis. Such plots can be used, for example, to estimate the intrinsic solubility (Avdeef, 1998). The difference curve is a plot of $\bar{n}_H$, the average number of bound protons, versus $p_cH(-\log[H^+])$. By measuring the pH, and after converting it into p_cH (Avdeef and Bucher, 1978), one knows the *free* (*unbound*) hydrogen ion concentration. The *total* hydrogen ion excess concentration in solution is defined by [HCl], [KOH], and by the dissociable protons, *n*, the sample substance brings to the solution. The difference between the *total* and the *unbound* concentrations is equal to the concentration of the *bound* hydrogen ions. The latter concentration divided by

that of the sample substance, C, gives the average number of bound hydrogen ions per molecule of substance, $\bar{n}_H$. That is,

$$\bar{n}_H = ([HCl] - [KOH] + nC - [H^+] + K_w/[H^+])/C \quad (15)$$

where K_w is the ionization constant of water (1.78×10^{-14} at 25°C, 0.15 M ionic strength).

3.5. Potentiometric refinement of solubility constants

The approximate equilibrium constants, determined by Bjerrum analysis, produce the 'seed' values for the iterative least-squares procedure for $\log S_0$ refinement, using the processing program, *p*S. The refined values are those which produce a minimum in the sum of the weighted squares of residuals:

$$R = \Sigma_i^{No} (pH_i^{obs} - pH_i^{calc})^2/\sigma_i^2(pH) \quad (16)$$

N_0 is the number of pH measurements; σ_i^2 is the estimated variance in the measured pH_i^{obs}. The model equation, pH_i^{calc}, is a function of the equilibrium constants, as well as the independent variables. The weighting scheme used in Eq. (16) is constructed from the variances (Avdeef, 1983)

$$\sigma^2(pH) = \sigma_c^2 + (\sigma_v\, dpH/dV)^2 \quad (17)$$

With the *p*SOL instrument, $\sigma_c = 0.005$ (units of pH), the fixed contribution to the variance in the measured pH, and $\sigma_v = 3\times10^{-5}$ ml, the estimated standard deviation in the volume of titrant. After each iterative cycle a test of the progress of refinement is indicated by the goodness-of-fit, GOF, which is defined by

$$GOF = [R/(N_0 - N_R)]^{1/2} \quad (18)$$

where N_R is the number of refined parameters. A GOF value of 1 is ideal in simple titrations in the absence of precipitation. Analyses of data taken from titrations of saturated solutions generally have higher values, indicating the presence of unidentified systematic errors in the pH measurements.

4. Results and discussion

4.1. Dissolution titration template (DTT)

We select propoxyphene hydrochloride to illustrate the structure of a typical template created (using the pK_a 9.06 and $\log P_{ow}$ 4.37) at the start of a dissolution titration. Fig. 2 shows a simulated titration curve. The high-pH region indicated with solid symbols (zones A and B in Fig. 2) corresponds to the anticipated region of precipitation; open symbols indicate the expected domain of complete dissolution (zones B′, C, D). Ideally, titrations begin in zone A. However, the very sparingly soluble sample is first taken to zone D (pH 3 in the example) until completely dissolved (which takes very little time); after that, the pH is adjusted to the starting value of 10.5 (zone A), where re-precipitation commences rapidly. These are helpful preliminary steps for samples which wet very poorly due to low solubility, and the steps are not needed if predicted $S_0 > 0.5$ mg/ml or if wetting is anticipated not to be a problem. (Without this step, we sometimes see crystals floating on top of the solution, evading the titration almost entirely).

The instrument recommends, based on the value of $\log P_{ow}$, that the total titration time be about 7.3 h in the case of propoxyphene. However, the time spent collecting each titration point is not evenly allocated. At the start of zone A, the suspension is first stirred for 40 min (longer times would be automatically calculated for less soluble samples). This step is meant to ensure that the initially formed (possibly amorphous-state) precipitate has an opportunity to turn into a more-stable crystalline state. At this stage, we typically observe the turbid solutions turning virtually clear, as tiny crystals deposit on the electrode pH-sensing bulb surface, or the quartz dispenser tip, or float on the surface of the solution, or crawl the walls of the sample vial via the meniscus. The deposit of the crystals on the bulb of the electrode does not appear to interfere with the pH measurements. However, crystallization on top of the frit reference junction could be a problem with conventional design electrodes. The use of annular ring type reference junctions is helpful in this regard.

Data in zone A are meant to be collected at a moderate speed. Since at high pH the dissolving solid is a nonionizing free base, minimal indications of the dissolution process are observed by the pH electrode. This region does not produces the most useful data for characterizing the intrinsic solubility in the DTT method. One is merely titrating water, so to speak. On the other hand, zone B (about 0.8 pH unit above the point of complete dissolution) is sufficiently lower in pH that the dissolving free base undergoes ionization, with an added effect on the pH. In the titration, this is an information-rich zone, and care is exercised in collecting precise data. This includes slowing down the data collection rate. The zone A data in the propoxyphene example are collected at the rate of about 0.56 pH/h, while zone B data are collected at the rate of 0.24 pH/h. At the end of zone B, one expects the slowest rate of dissolution, according to the kinetics model used in the study (see next section).

Since our estimate of the point of complete dissolution is no more precise than the accuracy of the prediction Eq. (14), zone B is extended (to zone B′) beyond the point of expected complete dissolution by about 0.2 pH unit, to serve as a confidence factor. Data in the post-dissolution zones B′ and C are also collected slowly. In zone B′, the rate continues at 0.24 pH/h and in zone C (which extends from the end of zone B′ to about one pH unit beyond complete dissolution), the rate increases to about 1.3 pH/h

in the case of propoxyphene. The template model assumes all solid has been dissolved by the time zone D is entered, and data acquisition is as rapid as that used with ordinary titrators, namely, about 14 pH/h.

If the template is based on a highly inaccurate set of estimated constants, the titration data may be collected too quickly or too slowly. Nevertheless, the data are usually of sufficiently adequate quality for processing to obtain approximate solubility constants. These constants are then used in a repeated titration, with a much-improved template.

This unusual DTT data collection strategy is the iteratively improved heuristic result of applying the kinetics model in such a way that just enough time is allocated to collecting data to ensure that dissolution essentially reaches equilibrium at each point in the titration.

4.2. Diffusion layer and bulk solution concentrations

We chose propoxyphene to further illustrate the DTT method. Fig. 3b shows the Bjerrum plots of the three titrations performed with propoxyphene. With 0.1–0.7 mM samples, ionization of the free base commences below pH 9.5, as indicated by $\bar{n}_H$ values ascending from zero. Complete dissolution takes place in the region pH 7.3–8.3,

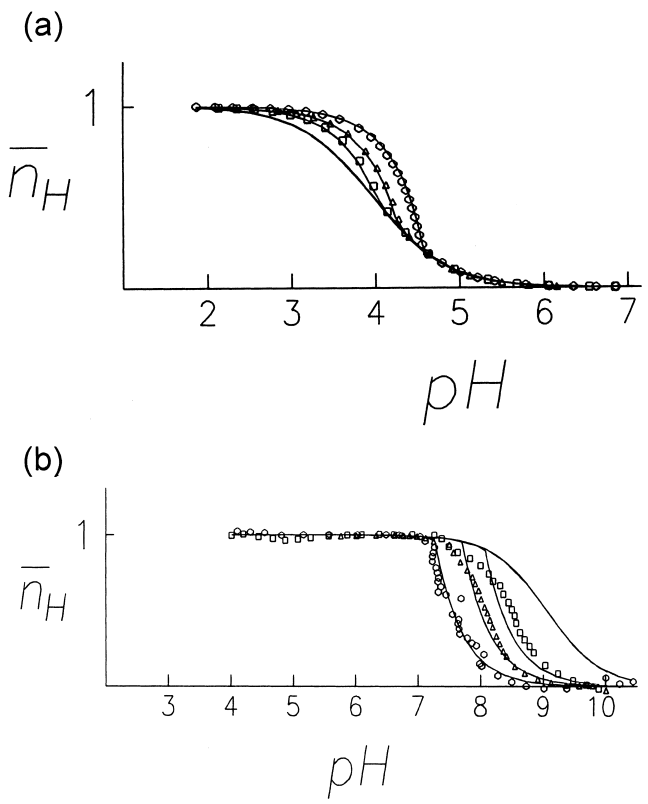

Fig. 3. Bjerrum plots: (a) benzoic acid, indicating ideal behaviour (squares, 96 mM; triangles, 130 mM; hexagons, 500 mM), and (b) propoxyphene hydrochloride, showing some incomplete dissolution (squares, 0.11 mM; triangles, 0.25 mM; hexagons, 0.73 mM).

depending on the actual amount of sample used. The $\bar{n}_H$ values are near one by then.

To illustrate the kinetics model calculations of Eq. (13), we elected to simulate the titration condition of 0.25 mg propoxyphene HCl added to 1.00 ml of 0.15 M KCl. The pH region of most interest is where the Bjerrum function changes from about 0.1 to about 0.9 (pH 7.3–9.0). Table 1 lists the equilibrium concentrations of species in the three states described in Section 2: the initial state, Σ_i, the state at the surface of the solid in contact with solution, Σ_0, and the state at the outer boundary of the diffusion layer, Σ_h. The states Σ_i and Σ_0 were selected to be precisely 0.1 pH units apart, which is a typical spacing of data points in a titration curve. Concentrations of species and total reactant concentrations at pH 9.0 ($\bar{n}_H$ 0.020), 8.5 ($\bar{n}_H$ 0.062), 8.0 ($\bar{n}_H$ 0.204), 7.5 ($\bar{n}_H$ 0.637), and 7.32 ($\bar{n}_H$ 0.977, near the point of complete dissolution) were calculated with *p*S.

The gradient concentrations listed in the right-most column in Table 1 provide the driving forces for the diffusion-controlled process of dissolution. The initial dissolution flux may be estimated from Eq. (13), and should be directly proportional to the change in the total propoxyphene concentration, $T_B^0 - T_B^h$, which is precisely the same as $T_B^0 - T_B^i$. From Table 1, the latter total concentration change (in units of 10^{-7} mol/cm^3) follows the trend 0.03 (pH 9.0), 0.09 (pH 8.5), 0.29 (pH 8.0), 0.90 (pH 7.5) and 1.35 (pH 7.32). Clearly, the dissolution flux increases as pH decreases, since propoxyphene is more soluble at lower pH. However, the actual rate of dissolution depends on the available surface area, as indicated by Eq. (13). Just as the flux increases, the area decreases, most dramatically near the point of complete dissolution.

We attempted to make the quantitative estimates of the above two opposing tendencies, by postulating that the solid consist of 10-μm spheres of unit density. This corresponds to specific surface area of 0.6 m^2/g. We chose the spherical shape to simplify calculations. (Since we did not actually measure the specific surface area, the calculations can only be approximate, *used to suggest trends*. In the design of the DTT algorithm, that was sufficient). We further assumed that the diffusivity of propoxyphene can be estimated from an expression based on inverse cube-root of partial molar volume (Flynn et al., 1974) to be about 5×10^{-6} cm^2/s, and that the thickness of the diffusion layer is about 3×10^{-3} cm. These estimates seem reasonable. Table 2 lists the results of applying the above approximations and the precise equilibrium concentrations from Table 1 to the rate expression Eq. (13). Of interest is the estimate of the rate of dissolution in the various zones of the titration. At pH 9 (zone A), the rate is slow, at 0.07 (units of 10^{-10} mol/s). The titrator does not spend much time collecting these data, since the dissolved drug build up has little effect on the measured pH. The rate more than doubles from pH 9 to 8.5. This is driven largely by the increase in solubility (9–20 μg/ml), with minimal decrease in surface area. However, in the region pH 8–7.5,

Table 1
Diffusion layer and bulk solution concentrations[a]

Concentration	Σ_i (initial)	Σ_h ($x=h$) (perturbed)	Σ_0 ($x=0$) (final)	$\Sigma_0-\Sigma_i$ (net)	$\Sigma_0-\Sigma_h$ (gradient)
pH	9.10	8.96	**9.00**	−0.10	0.04
[B]	0.0977	0.0816	0.0977	0.0000	0.0108
[BH^+]	0.1096	0.1256	0.1380	0.0284	0.0161
[HCO_3^-]	0.1403	0.1449	0.1439	0.0036	−0.0010
[H_2CO_3]	0.0004	0.0005	0.0005	0.0001	−0.0000
[H^+]	0.0000	0.0000	0.0000	0.0000	−0.0000
[OH^-]	0.1766	0.1288	0.1400	−0.0366	0.0112
T_B	0.2073	0.2073	0.2358	0.0284	**0.0284**
T_H	0.0737	0.1423	0.1423	0.0686	0.0000
pH	8.60	8.13	**8.50**	−0.10	0.37
[B]	0.098	0.039	0.098	0.000	0.059
[BH^+]	0.346	0.406	0.434	0.088	0.027
[H^+]	0.000	0.000	0.000	0.000	−0.000
[OH^-]	0.056	0.019	0.045	−0.011	0.026
T_B	0.44	0.44	0.53	0.09	**0.09**
T_H	0.45	0.55	0.55	0.10	0.00
pH	8.10	5.52	**8.00**	−0.10	2.48
[B]	0.098	0.000	0.098	0.000	0.097
[BH^+]	1.096	1.194	1.380	0.284	0.186
[H^+]	0.000	0.037	0.000	0.000	−0.037
[OH^-]	0.018	0.000	0.014	−0.004	0.014
T_B	1.19	1.19	1.48	0.29	**0.29**
T_H	1.24	1.53	1.53	0.29	0.0
pH	7.60	4.28	**7.50**	−0.10	3.22
[B]	0.098	0.000	0.098	0.000	0.098
[BH^+]	3.436	3.532	4.335	0.899	0.803
[H^+]	0.000	0.643	0.000	0.000	−0.642
[OH^-]	0.006	0.000	0.004	−0.001	0.004
T_B	3.53	3.53	4.43	0.90	**0.90**
T_H	3.60	4.50	4.50	0.90	0.0
pH	7.42	4.05	**7.32**	−0.10	3.27
[B]	0.098	0.000	0.098	0.000	0.098
[BH^+]	5.210	5.309	6.561	1.351	1.252
[H^+]	0.000	1.104	0.001	0.000	−1.103
[OH^-]	0.004	0.000	0.003	−0.001	0.003
T_B	5.31	5.31	6.66	1.35	**1.35**
T_H	5.38	6.73	6.73	1.35	0.0

[a] Calculations based on propoxyphene (B): 25°C, 250 μg hydrochloride salt added to 1.00 ml 0.15 M KCl, containing 0.016 mM CO_2. Direct concentration in units of 10^{-7} mol/cm^3. Σ is a symbol used to designate a conditional equilibrium state (see text). The HCl titrant dose (τ, see text) needed to take Σ_i to Σ_0 is given by $T_H^0-T_H^i$. The carbon dioxide was added to the model at a concentration often found in solubility measurements by the DTT method. The carbonate species concentrations are shown at pH 9, to illustrate their effect on the other total and reactant concentrations.

Table 2
Simulated dissolution rates during titration of propoxyphene

pH_0	S (μg/ml)	(dm_B/dt)/A[a] (mol/cm^2 s $\times10^{10}$ $=J_{total}$)	ppt. wt.[b] (μg)	A[c] (cm^2)	dm_B/dt (mol/s $\times10^{10}$)	Equilib. time for ΔpH 0.1 (h)	'Shake-flask' time (h)
11.0	3.7 (intrinsic)	0.0005	246.3	1.48	0.00075	0.074	36.5
9.0	8.9	0.05	241.1	1.44	0.07	0.119	0.91
8.5	19.9	0.14	230.1	1.38	0.19	0.127	0.71
8.0	55.5	0.47	194.5	1.16	0.54	0.144	0.59
7.5	166.5	1.50	83.5	0.50	0.75	0.332	0.55
7.32	249.6	2.33	0.4	0.002	0.005	75.2	0.49

[a] Used $D_B=5\times10^{-6}$ cm^2/s and $h=3\times10^{-3}$ cm in Eq. (12).
[b] Total amount of sample was 250 μg in 1.00 ml 0.15 M KCl.
[c] A=powder surface area available for dissolution; assumed to be that of 10-μm spherical particles of unit density (0.6 m^2/g).

the increase in solubility is nearly equally offset by the decrease in available surface. The dissolution rate reaches its maximum value of about 0.5–0.75 just in the region of the titration where the data are most sensitive to the determination of the intrinsic solubility constant by the pH-metric method (namely, where the Bjerrum function is near 0.5).

As the point of complete dissolution approaches, the rate again decreases to very low values, as expected from even the simple Noyes–Whitney equation (Eq. (1)). In actual propoxyphene titrations, as indicated by the Bjerrum plots in Fig. 3b, the incompleteness of dissolution can be readily recognized by the departure of points from the best-fit line near the region of the expected complete dissolution, especially noticeable in the two right-most curves ($\bar{n}_H > 0.8$), associated with the lowest sample concentrations. This is expected from the kinetics analysis. Usually, these few points are assigned zero weights in the weighted nonlinear least-squares refinement. It is interesting to explore the relationship between the two integration constants, C_1 and C_2 (Eqs. (10) and (11)). The gradients across the diffusion layer appearing in the two expressions can be obtained from Table 1. Careful examination of concentrations, for example at pH 9, indicates that the *two constants would only be the same, had all diffusivities in the example been equal*. Such would be the case from the equality

$$([B]_0 - [B]_h)/h = ([H^+]_0 - [H^+]_h)/h - ([OH^-]_0 - [OH^-]_h)/h \quad (19)$$

This is approximately true for pH near 7, but in general this is false, since diffusivities of typical samples (MW 300) are four to five times lower than those of the hydrogen and hydroxide ions. The penultimate column in Table 2 lists the estimated total time for the dissolution to reach near equilibrium assuming the initial flux rate applies to titrant perturbations resulting in 0.1 pH unit changes. The times are nearly constant from pH 11 to 8. (It is noteworthy that 0.1 pH shifts lead to increasingly larger quantities of sample dissolving: 0.008 μg at pH 11, 1.1 μg at pH 9, 3.3 μg at pH 8.5, 11 μg at pH 8.0, 34 μg at pH 7.5, 51 μg at pH 7.32.) The last column in Table 2 lists the estimated equilibrium times for a shake-flask experiment, assuming same quantities of material and sink conditions. The times near the high pH where intrinsic solubility would be characterized by the traditional method can indeed be of the order of one to several days, as our approximate analysis indicates. However, the titration method is not bound by this time requirement. The method produces information about the intrinsic solubility most effectively from the region where the Bjerrum function is about 0.5 (Avdeef, 1998), where equilibrium times are of the order of minutes! This is a very important practical characteristic that distinguishes the time requirements of the traditional method from the new pH-metric DTT method.

4.3. Bjerrum analysis: graphical indications of incomplete dissolution

Bjerrum plots of propoxyphene are presented in Fig. 3b. Such plots not only are used to estimate intrinsic solubility constants, as thoroughly explored elsewhere (Avdeef, 1998), they can be used to recognize regions in the data which suffer from the effects of incomplete dissolution. Fig. 3a depicts the case of benzoic acid, which is shown to illustrate a well-behaved system. Three separate titrations are depicted, with each curve displaced from the reference curve (no precipitate) by an amount proportional to the quantity of substance used.

Fig. 3b corresponds to three different titrations of propoxyphene. The left-most shifted curve corresponds to the highest concentration (0.72 mM, Table 3) and is one least affected by systematic errors. The other two curves, at lower concentrations, noticeably bend away from the best-fit solid curves near pH 8.0 and 8.4, for $\bar{n}_H > 0.75$. It appears that not enough time had been allotted to these points for the pH to rise to equilibrium values. We cope with this shortcoming by recognizing that the aberrant region (indicated by highest weighted residuals in the least-squares refinement), which requires a very prolonged equilibration, is unsuitable for refinement analysis, and thus we exclude the points in that region from refinement (in effect assigning zero weights to those points).

4.4. Refined intrinsic solubility constants, S_0, and solubilities at selected pH

Table 3 summarizes the titration conditions used in the study. Table 4 lists the refined intrinsic solubilities and the solubilities at several selected pH values of the compounds studied here, along with some comparisons to the literature.

Diltiazem hydrochloride in one of the titrations hydrolyzed at high pH. We were able to quantitate the extent of hydrolysis to be 18%, from the in situ titration of the acetic

Table 3
Potentiometric titrations

Compound	No. titrations	Conc. range (mM)	Assay time (h)	Group GOF
Benzoic Acid	7	3–501	1–11	2.5
Cimetidine	3	93–280	4–15	2.7
Diltiazem HCl	2	7, 16	6, 22	5.9
Enalapril Maleate	2	62, 618	3, 16	2.6
Metoprolol Tartrate	4	53–156	4–6	1.2
Nadolol	3	213–238	11–13	3.9
Propoxyphene HCl	5	0.12–0.72	4–7	17.0
Quinine HCl	4	0.12–7.2	6–7	2.3
Terfenadine	5	0.02–0.15	3–5	1.1
Trovafloxacin mesylate	2	1.1, 2.9	5–7	4.2

Table 4
Intrinsic solubilities and solubilities at selected pH values[a]

Compound	Solubility at selected pH values				S_0 (intrinsic)	$\log(1/S_0)$ (mol/l)	log P	pK_a	Lit.
	pH 1.0	pH 5.0	pH 6.8	pH 7.4					
Benzoic acid	3.2 mg/ml	29 mg/ml	1.8 g/ml	7.2 g/ml	3.2 mg/ml	1.59 ±0.02	1.96	3.99	3.34 mg/ml[b]
Cimetidine		1.0 g/ml	24 mg/ml	13 mg/ml	9.3 mg/ml	1.43 ±0.08	0.48	6.93	6.0 mg/ml[c]
Diltiazem HCl			10 mg/ml	3.0 mg/ml	0.51 mg/ml	2.95 ±0.08	2.89	8.02	
Enalapril maleate	3.3 g/ml	24 mg/ml	430 mg/ml	1.7 g/ml	21 mg/ml	1.36 ±0.08	0.16	5.42, 2.92	25 mg/ml[e]
Metoprolol tartrate				10 g/ml	43 mg/ml	1.20 ±0.08	1.96[e]	9.56[d] tartrate: 3.88, 2.80[d]	
Nadolol					8.3 mg/ml	1.57 ±0.08	0.85	9.69	
Propoxyphene HCl			0.83 mg/ml	0.21 mg/ml	3.7 μg/ml	5.01 ±0.12	4.37	9.06	
Quinine HCl			33 mg/ml	8.0 mg/ml	550 μg/ml	2.82 ±0.02	3.50[j]	8.53, 4.26[f]	570 μg/ml(22°)[g]
Terfenadine		85 μg/ml	63 μg/ml	16 μg/ml	97 ng/ml	6.69 ±0.17	5.72	9.53	10 μg/ml[h]
Trovafloxacin mesylate		139 μg/ml	18 μg/ml	19 μg/ml	15 μg/ml	4.53 ±0.06	0.13	8.03, 5.87	15 μg/ml[i]

[a] 25°C, 0.15 M KCl medium.
[b] Yalkowsky and Dannenfelser (1998), average of 16 values of water solubility, unspecified pH.
[c] Flynn et al. (1974).
[d] Dehn (1917).
[e] Ip and Brenner (1990).
[f] Avdeef and Box (1996, pp. 88, 128).
[g] Dehn (1917).
[h] Badwan et al. (1990).
[i] C. Lipinski, private communication (1998).

acid byproduct. By reversing the direction of titration, the hydrolysis was completely avoided.

The selection of compounds studied here ranged in intrinsic solubilities from a high of 43 mg/ml (metoprolol tartrate) to a low of 97 ng/ml (terfenadine). With the exception of benzoic acid and quinine hydrochloride, all molecules possess some difficulty to the design of the experiments. We considered these molecules the 'trainer' set for the DTT method.

5. Conclusion

The new automated DTT potentiometric method is about an order of magnitude faster than the traditional saturation shake-flask methods at determining equilibrium solubility–pH profiles of ionizable compounds. What may take days do by one can be done in hours by the other. This was demonstrated in practice and supported by a model derived from modern dissolution theory applied to acid–base titrations. The DTT method may be very useful in pre-formulation applications, and perhaps in discovery applications, where it can be used to validate computational prediction methods and also measurement of solubility by high-throughput methods (Avdeef, 2001).

Acknowledgements

We are grateful to William M. Meylan (Syracuse Research Corp.) and Charles Brownell (FDA, Rockville, MD) for drawing our attention to critical literature references. Christopher Lipinski (Pfizer, Groton, CT) was kind to provide the trovafloxacin mesylate we used. Special thanks go to Melissa A. Strafford and Konstantin Tsinman (*p*ION) for assisting with some of the experiments and checking some of the derivations.

References

Attwood, D., Gibson, J., 1978. Aggregation of antidepressant drugs in aqueous solution. J. Pharm. Pharmacol. 30, 176–180.

Avdeef, A., Bucher, J.J., 1978. Accurate measurements of the concentration of hydrogen ions with a glass electrode: calibrations using the Prideaux and other universal buffer solutions and a computer-controlled automatic titrator. Anal. Chem. 50, 2137–2142.

Avdeef, A., 1983. Weighting scheme for regression analysis using pH data from acid-base titrations. Anal. Chim. Acta 148, 237–244.

Avdeef, A., 1985. STBLTY: Methods for construction and refinement of equilibrium models. In: Leggett, D.J. (Ed.), Computational Methods for the Determination of Formation Constants. Plenum, New York, pp. 355–474.

Avdeef, A., Box, K.J., 1996. In: Sirius Technical Application Notes, Vol.

2. Sirius Analytical Instruments Ltd, Forest Row, E. Sussex, UK, ISBN 1-901125-05X.

Avdeef, A., 1998. pH-Metric solubility. 1. Solubility–pH profiles from Bjerrum plots, Gibbs buffer and pK_a in the solid state. Pharm. Pharmacol. Commun. 4, 165–178.

Avdeef, A., Berger, C.M., Brownell, C., 2000. pH-Metric solubility. 2. Correlation between the acid-base titration and the saturation shake-flask solubility–pH methods. Pharm. Res. 17, 85–89.

Avdeef, A., 2001. High-throughput measurements of solubility profiles. In: Testa, B., van de Waterbeemd, H., Folkers, G., Guy, R. (Eds.), Pharmacokinetic Optimization in Drug Research. Verlag Helvetica Chimica Acta and Wiley–VCH, Zürich and Weinheim, pp. 305–326.

Badwan, A.A., Alkaysi, H.N., Owais, L.B., Salem, M.S., Arafat, T.A., 1990. Terfenadine. Anal. Profiles Drug Subst. 19, 627–662.

Bogardus, J.B., Blackwood, Jr. R.K., 1979. Solubility of doxycycline in aqueous solution. J. Pharm. Sci. 68, 188–194.

Brünner, E., 1904. Reaktionsgeschwindigkeit in heterogenen systemen. Z. Phys. Chem. 47, 56–102.

Charykov, A.K., Tal'nikova, T.V., 1974. pH-Metric method of determining the solubility and distribution ratios of some organic compounds in extraction systems. J. Anal. Chem. USSR 29, 818–822.

Dehn, W.M., 1917. Comparative solubilities in water, in pyridine and in aqueous pyridine. J. Am. Chem. Soc. 39, 1399–1404.

Faller, B., Wohnsland, F., 2001. Physicochemical parameters as tools in drug discovery and lead optimization. In: Testa, B., van de Waterbeemd, H., Folkers, G., Guy, R. (Eds.), Pharmacokinetic Optimization in Drug Research. Verlag Helvetica Chimica Acta and Wiley–VCH, Zürich and Weinheim, pp. 257–274.

FDA Guidance for Industry Waiver of In Vivo Bioavailability and Bioequivalence Studies for Immediate Release Solid Oral Dosage Forms Containing Certain Active Moieties/Active Ingredients Based on a Biopharmaceutics Classification System. CDERGUID\2062dft.wpd Draft, Jan. 1999(www.fda.gov/cder/guidance/2062dft.pdf)

Flynn, G.L., Yalkowsky, S.H., Roseman, T.J., 1974. Mass transport phenomena and models: theoretical concepts. J. Pharm. Sci. 63, 479–510, (Fig. 6).

Higuchi, T., Shih, F.-M.L., Kimura, T., Rytting, J.H., 1979. Solubility determination of barely aqueous soluble organic solids. J. Pharm. Sci. 68, 1267–1272.

Ip, D.P., Brenner, G.S., 1990. Enalapril maleate. Anal. Profiles Drug Subst. 19, 225–227.

Kaufman, J.J., Semo, N.M., Koski, W.S., 1975. Microelectrometric titration measurement of the pK_as and partition and drug distribution coefficients of narcotics and narcotic antagonists and their pH and temperature dependence. J. Med. Chem. 18, 647–655.

Ledwidge, M.T., Corrigan, O.I., 1998. Effects of surface active characteristics and solid state forms on the pH solubility profiles of drug-salt systems. Int. J. Pharm. 174, 187–200.

Levy, R.H., Rowland, M., 1971. Dissociation constants of sparingly soluble substances: nonlogarithmic linear titration curves. J. Pharm. Sci. 60, 1155–1159.

Miyazaki, S., Oshiba, M., Nadai, T., 1981. Precaution on use of hydrochloride salts in pharmaceutical formulation. J. Pharm. Sci. 70, 594–596.

Mooney, K.G., 1980. Dissolution Kinetics of Organic Acids. Ph.D. Dissertation, University of Kansas.

Mooney, K.G., Mintun, M.A., Himmelstein, K.J., Stella, V.J., 1981a. Dissolution kinetics of carboxylic acids. I: Effect of pH under unbuffered conditions. J. Pharm. Sci. 70, 13–22.

Mooney, K.G., Mintun, M.A., Himmelstein, K.J., Stella, V.J., 1981b. Dissolution kinetics of carboxylic acids. II: Effects of buffers. J. Pharm. Sci. 70, 22–32.

Nernst, W., 1904. Theorie der reaktionsgeschwindigkeit in heterogenen systemen. Z. Phys. Chem. 47, 52–55.

Noyes, A.A., Whitney, W.R., 1897. The rate of solution of solid substances in their own solutions. J. Am. Chem. Soc. 19, 930–934.

Ritschel, W.A., Alcorn, G.C., Streng, W.H., Zoglio, M.A., 1983. Cimetidine-theophylline complex formation. Methods Find. Exp. Clin. Pharmacol. 5, 55–58.

Roseman, T.J., Yalkowsky, S.H., 1973. Physicochemical properties of prostaglandin $F_{2\alpha}$ (tromethamine salt): solubility behavior, surface properties, and ionization constants. J. Pharm. Sci. 62, 1680–1685.

Serajuddin, A.T.M., Jarowski, C.I., 1985a. Effect of diffusion layer pH and solubility on the dissolution rate of pharmaceutical bases and their hydrochloride salts I: phenazopyridine. J. Pharm. Sci. 74, 142–147.

Serajuddin, A.T.M., Jarowski, C.I., 1985b. Effect of diffusion layer pH and solubility on the dissolution rate of pharmaceutical bases and their hydrochloride salts II: salicylic acid, theophylline, and benzoic acid. J. Pharm. Sci. 74, 148–154.

Strafford, M.A., Avdeef, A., Artursson, P., Johansson, C.A.S., Luthman, K., Brownell, C.R., Lyon, R., 2000. Determination of drug solubility using a potentiometric acid-base titration method compared to the saturation shake-flask method. In: 15th Ann. Meet., Am. Assoc. Pharm. Sci., Indianapolis.

Streng, W.H., Zoglio, M.A., 1984. Determination of the ionization constants of compounds which precipitate during potentiometric titration using extrapolation techniques. J. Pharm. Sci. 73, 1410–1414.

Streng, W.H., Yu, D.H.-S., Zhu, C., 1996. Determination of solution aggregation using solubility, conductivity, calorimetry, and pH measurements. Int. J. Pharm. 135, 43–52.

Todd, D., Winnike, R.A., 1994. A rapid method for generating pH-solubility profiles for new chemical entities. In: Abstr. 9th Ann. Meet., Am. Assoc. Pharm. Sci., San Diego.

Venkatesh, S., Li, J., Xu, Y., Vishnuvajjala, R., Anderson, B.D., 1996. Intrinsic solubility estimation and pH-solubility behavior of cosalane (NSC 658586), and extremely hydrophobic diprotic acid. Pharm. Res. 13, 1453–1459.

Weiss, T.F., 1996. In: Cellular Biophysics, Vol. 1. MIT Press, Cambridge, MA, p. 124.

Yalkowsky, S.H., Banerjee, S., 1992. In: Aqueous Solubility: Methods of Estimation for Organic Compounds. Marcel Dekker, New York, pp. 58–68.

Yalkowsky, S.H., Dannenfelser, R.-M. (Eds.), 1998. AQUASOL dATAbASE of Aqueous Solubility, 5th Edition. College of Pharmacy, Univ. Arizona, Tucson, AZ 85721.